Acta Med. Okayama, 2003
Vol. 57, No. 4, pp. 163-170

Acta Medica Okayama
http://www.lib.okayama-u.ac.jp/www/acta/

Original Article

Differential Diagnosis of Adrenal Masses by Chemical Shift and Dynamic Gadolinium Enhanced MR Imaging

Nobuya Sasai*, Izumi Togami, Masatoshi Tsunoda, Tetsuro Sei, Shiro Akaki, and Yoshio Hiraki

Department of Radiology, Okayama University Graduate School of Medicine and Dentistry, Okayama 700-8558, Japan

Chemical shift MRI is widely used for identifying adenomas, but it is not a perfect method. We determined whether combined dynamic MRI methods can lead to improved diagnostic accuracy. Fifty-seven adrenal masses were examined by chemical shift and dynamic MR imaging using 2 MR systems. The masses included 38 adenomas and 19 non-adenomas. In chemical shift MRI studies, the signal intensity index (SI) was calculated, and the lesions classified into 5 types in the dynamic MRI studies. Of the 38 adenomas studied, 37 had an SI greater than 0. In the dynamic MRI, 34 of 38 adenomas showed a benign pattern (type 1). If the SI for the adenomas in the chemical shift MRI was considered to be greater than 0, the positive predictive value was 0.9, and the negative predictive value was 0.94 and $\kappa = 0.79$. If type 1 was considered to indicate adenomas in the dynamic MRI, the corresponding values were 0.94, 0.81 and $\kappa = 0.77$ respectively. The results obtained when the 2 methods were combined were 1, 0.95 and $\kappa = 0.96$ respectively. The chemical shift MRI was found to be useful for identifying adenomas in most cases. If the adrenal mass had a low SI ($0 < SI < 5$), dynamic MRI was also found to be helpful for making a differential diagnosis.

Key words: adrenal adenoma, MRI, contrast media

Adrenal masses are often detected during abdominal CT examinations. Benign non-functioning adenomas are found by CT in 0.6% of the adult population [1]. Among cancer patients, 8.6%-27% have an adrenal metastasis at autopsy [2-4]. In 330 patients with non-small cell bronchogenic carcinoma, it was found that an isolated adrenal mass was more likely to be benign than metastatic [5]. The adrenal gland is therefore a common site for both benign and malignant masses. It is clinically important to distinguish adenomas from malignant masses, especially in cancer patients.

Malignant lesions have prolonged T1 and T2 relaxation times. A number of reports have suggested that adrenal masses can be histologically characterized based on the findings of T1- and T2-weighted MR imaging. When the cutoff value of the T2 relaxation time in the benign range (< 60 msec) was used, the overlap remained within 13% [6]. Overlap occurred in 35% of the T1-weighted SE images [7].

Recently, there have been some reports that chemical shift MR imaging is more useful for differentiating adrenal masses than other methods. Mitchell *et al.* [8] described the use of chemical shift MR imaging to differentiate benign adrenocortical masses from malignant masses. Benign adrenocortical masses often contain lipid, but metastases and pheochromocytomas do not. This distinction was found in 43 of 44 masses. The cutoff for discriminating between adenomas and other masses is a

Received December 3, 2002; accepted February 25, 2003.
*Corresponding author. Phone: +81-86-235-7315; Fax: +81-86-235-7316
E-mail: nsasai@mac.com (N. Sasai)

signal intensity index (SI) of 5% [9] or 3% [10], which means that an SI from 0% to 5% is considered an equivocal reading, in order to reduce false negatives. The SI is defined as the percentage of signal remaining in the opposed-phase image relative to the in-phase image.

Fast gradient echo imaging permits not only examination during suspended respiration with high image quality, but also the visualization of functional processes after the administration of a contrast agent. Adenomas exhibit moderate enhancement and rapid washout. Malignant masses and pheochromocytomas, on the other hand, show pronounced enhancement and a markedly slower washout. The degree of overlap is almost 10% [11, 12].

Both dynamic imaging and chemical shift MR imaging are useful for the differential diagnosis of adrenal masses, but these methods overlap to some degree, and the most effective application of these 2 methods has not yet been established. The purpose of the present study was to determine whether using both methods in combination could lead to an improvement in diagnostic accuracy.

Materials and Methods

Patients. Over a 6-year period (from February 1994 to July 2000), 53 patients (30 men and 23 women; age range, 30–84 years; mean age, 55.7 years) with 57 adrenal masses underwent MR imaging after the detection of an adrenal mass by CT. The masses included 38 adenomas (0.6–11 cm), 9 pheochromocytomas (2.8–7.5 cm), 6 metastases (2.3–3.8 cm), 2 myelolipomas (5.1 and 7.8 cm), 1 adrenocortical carcinoma (7.3 cm), and 1 lymphangioma (2 cm). The adenomas included 32 non-hyper functioning adenomas and 6 hyper functioning adenomas (3 with Cushing's disease, 3 with primary aldosteronism). The benign adrenal masses were surgically confirmed to be non-malignant in 10 masses, while the other masses underwent follow-up CT scanning at least 1 year later, with no changes observed in the sizes of these masses. The diagnosis was surgically confirmed in all masses with pheochromocytoma, myelolipoma, or adrenocortical carcinoma. One metastatic adrenal mass was confirmed at autopsy, while follow-up CT scans showed an increase in the size of the mass in the other masses. Of the metastatic lesions, 4 were from lung adenocarcinoma, and 2 from hepatocellular carcinoma.

MR imaging. The MR images were obtained with 1.5-T superconducting systems (MAGNETOM H15 and MAGNETOM Vision; Siemens Medical Systems, Erlangen, Germany). For the Vision system, the body-array coil was used in all cases, and for the H15 system, the body coil was used. In-phase and opposed-phase gradient-echo axial images were obtained during suspended respiration. For the H15 system, TR = 100 msec, TE = 13/11 msec (in-phase/opposed-phase), flip angle = 20°, and slice thickness = 5 mm. For the Vision system, TR = 100 msec, TE = 9/7 msec (in-phase/opposed-phase), flip angle = 30°, and slice thickness = 5 mm. For the Vision system, the double echo sequence to acquire both in-phase and opposed-phase images simultaneously were used in 11 cases. Dynamic MRI was used to obtain coronal images using a gradient-echo technique (FLASH 3D for the H15, FISP 3D for the Vision), with TR/TE = 5.8/2.8 msec, flip angle = 30°, and matrix = 168 × 256 (H15) or TR/TE = 5/2 msec, flip angle = 25°, and matrix = 128 × 256 with a fat saturation pulse in 27 cases (Vision). In each sequence, the respiration suspension time was 20–30 sec. The images were obtained before the intravenous administration of 0.1 mmol/kg of Gd-DTPA (Magnevist; Schering, Osaka, Japan) and then 4 times at 35 sec intervals after administration. Delayed images were also obtained about 5 min after administration.

Data Analysis. In the chemical shift MRI studies, the signal intensity index (SI) was calculated as follows: $SI = (S_{in}(A/S) - S_{opposed}(A/S))/S_{in}(A/S) \times 100$, where $S_{in}A$ is the signal intensity of the adrenal lesion on in-phase images, $S_{in}S$ is the signal intensity of the spleen on in-phase images, $S_{opposed}A$ is the signal intensity of the adrenal lesion on opposed-phase images, and $S_{opposed}S$ is the signal intensity of the spleen on opposed-phase images. An SI greater than 0 was assumed to indicate a benign lesion. In double echo sequences, it was not necessary to calculate a reference value (signal intensity of the spleen).

In the dynamic MRI studies, the lesions were classified into 5 types as follows:

1. rapid enhancement and rapid washout
2. rapid enhancement and slow washout
3. slow enhancement and slow washout
4. slow enhancement
5. no enhancement

Rapid enhancement was defined as the maximum enhancement observed before the second phase, and slow enhancement was defined as the maximum enhancement observed in a later phase. Rapid washout was defined as a signal intensity less than 80% of the maximum enhance-

ment in the delayed phase, and slow washout was defined as a signal intensity greater than 80% of the maximum enhancement in the delayed phase. Lesions classified as type 1 were assumed to be benign.

The regions of interest (ROIs) were set as large as possible while still being representative of the particular tissue. The ROIs were set up so that they might become as similar as possible between the in-phase and opposed-phase. In addition, the ROIs were set up so that the different phases of the dynamic MRIs could be measured. The ROIs were measured 3 times, and the 2 nearest values were averaged.

The positive predictive value and the negative predictive value for the adenomas of each method were calculated. The results of each method were quantified using the kappa statistic. Kappa statistic values greater than 0.7 typically indicated good agreement, whereas values between 0.4 and 0.7 reflected moderate agreement. We have studied further the usefulness of dynamic MRI over chemical shift MRI. If dynamic MRI is performed in mistaken results in chemical shift MRI, calculated same way as above. Differences in the diagnostic capabilities of the 2 MR systems employed were analyzed using the chi-squared test.

Results

In chemical shift MRI studies, the SI values were between −14 and 60 for adenomas, −16 to 18 for pheochromocytomas, −13 to −1 for metastases, −12 for cancer, 71 and 76 for myelolipomas, and 15 for lymphangioma (Fig. 1). Of the 38 adenomas studied, 37 had an SI greater than 0. One adenoma had an SI of −14 (Fig. 2). This mass was resected, and showed marked gray-red hemorrhagic degeneration, with tiny areas of yellow nodular adenoma seen in red areas of fresh hemorrhage. In dynamic MRI, this adenoma showed a malignant pattern (type 4) (Fig. 3).

In the dynamic MRI, 34 of the 38 adenomas showed rapid enhancement and rapid washout (type 1) (Table 1). Three adenomas that did not show a benign pattern on dynamic MRI showed a benign pattern in chemical shift MRI (SI = 7, 1, 9). The remaining adenoma had an SI of −14, as mentioned previously. Two metastases from HCC showed a benign pattern on the dynamic MRI (Figs. 4, 5). No other malignant masses showed a benign pattern.

If the SI for adenomas in chemical shift MRI is considered to be greater than 0, the positive predictive value is 0.9 (37 / 41), and the negative predictive value is 0.94 (15 / 16) and $\kappa = 0.79$. If type 1 is considered to indicate adenomas in dynamic MRI, the positive predictive value is 0.94 (34 / 36), and the negative predictive value is 0.81 (17 / 21) and $\kappa = 0.77$. If dynamic MRI is performed in mistaken chemical shift MRI results, the positive predictive value is 1 (37 / 37), and the negative predictive value is 0.95 (19 / 20) and $\kappa = 0.96$.

Three of the 4 adenomas with an SI in the equivocal range ($0 < SI < 5$) showed a benign pattern in dynamic MRI (Figs. 6, 7).

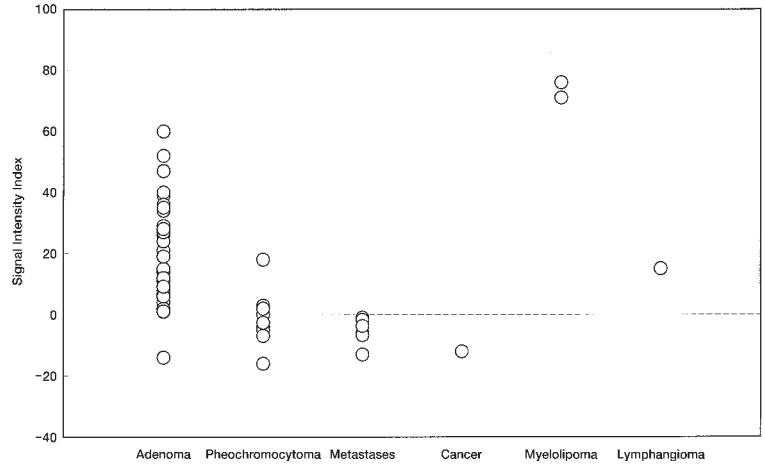

Fig. 1 Signal intensity index (SI) values of adrenal tumors. Of the 38 adenomas studied, 37 had an SI greater than 0.

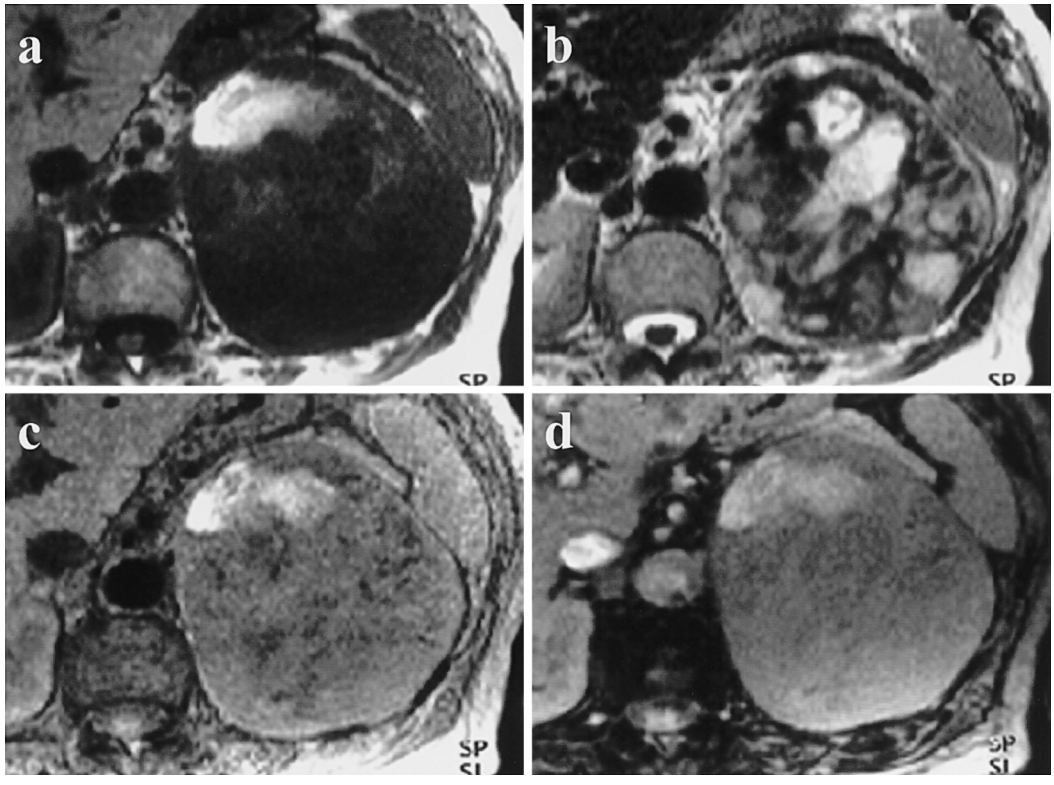

Fig. 2 Adenoma. T1-weighted (a) and T2-weighted (b) images show a heterogeneous tumor. The area of degeneration showed high signal intensity on the T2-weighted image. In-phase (c) and opposed-phase (d) gradient echo images are also shown. The opposed-phase image did not demonstrate low signal intensity compared with the in-phase image.

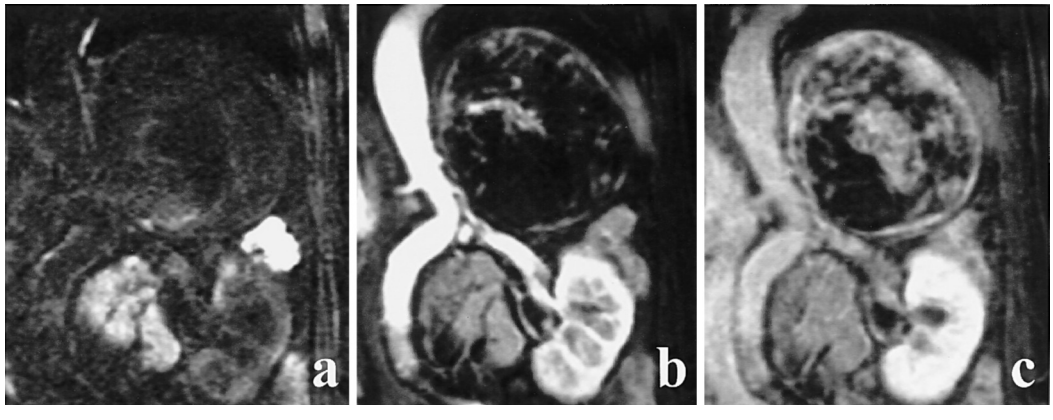

Fig. 3 Adenoma. Dynamic contrast-enhanced images show slow enhancement (Type 4) (before (a), early (b), and delayed (c)).

Table 1 Types in dynamic MRI for the differentiation of adrenal masses

	Type I	Type 2	Type 3	Type 4	Type 5
Adenoma	34		3	1	
Pheochromocytoma		3	3	3	
Metastases	2		1	3	
Cancer				1	
Myelolipoma				2	
Lymphangioma					1

Fig. 4 Metastasis from HCC. In-phase (a) and opposed-phase (b) gradient echo images and a subtraction image (c) show SI = −6.7 (malignant pattern). Post-contrast-enhanced image (d) shows slight enhancement.

Fig. 5 Metastasis from HCC. Dynamic contrast-enhanced images show Type I (before (a), early (b), and delayed (c)).

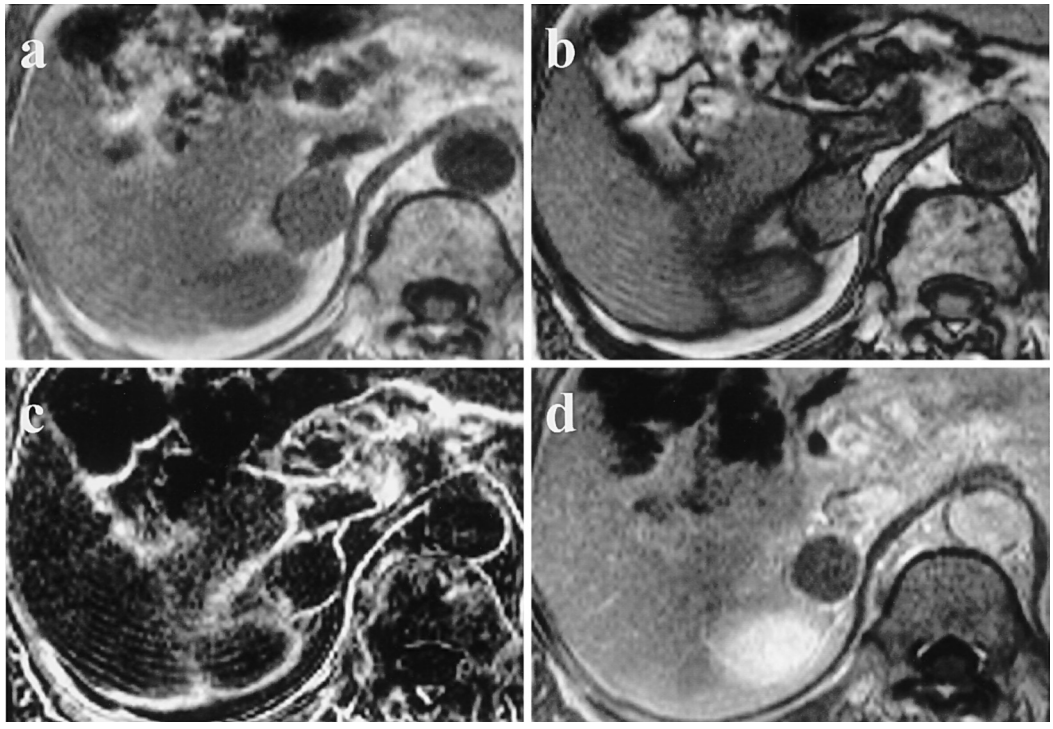

Fig. 4

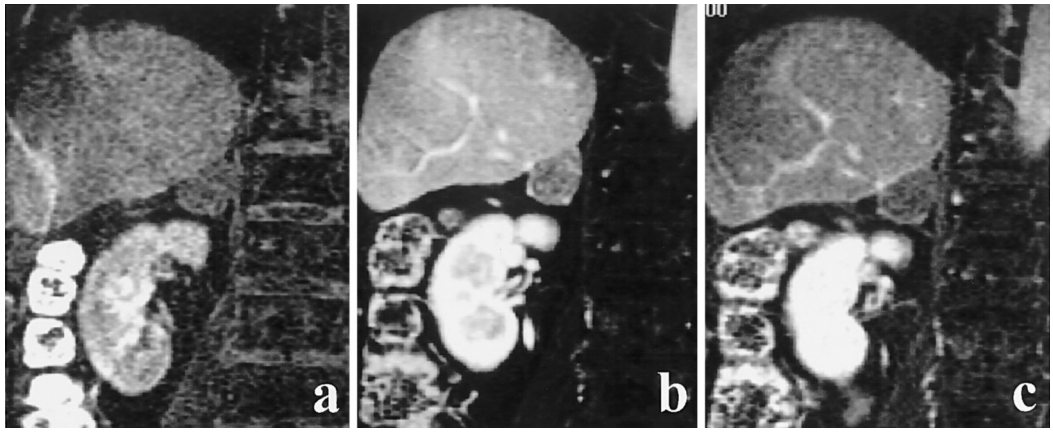

Fig. 5

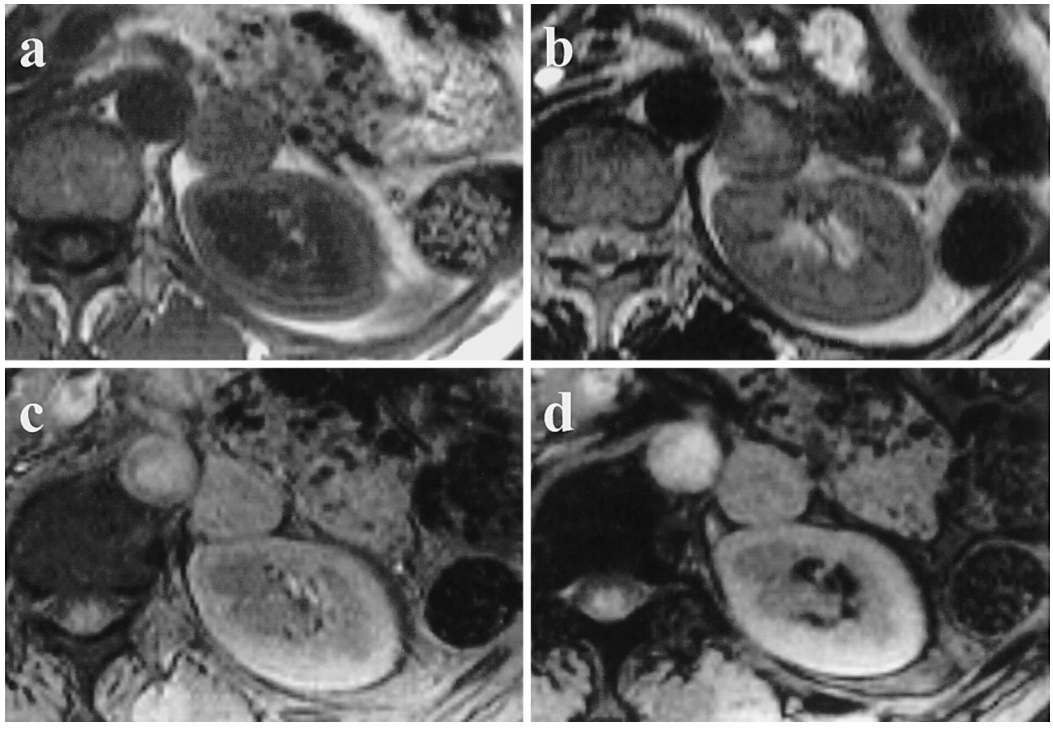

Fig. 6 Adenoma. T1-weighted (a) and T2-weighted (b) images demonstrate internal degeneration. In-phase (c) and opposed-phase (d) gradient echo images are also shown. The SI is 4 (gray zone).

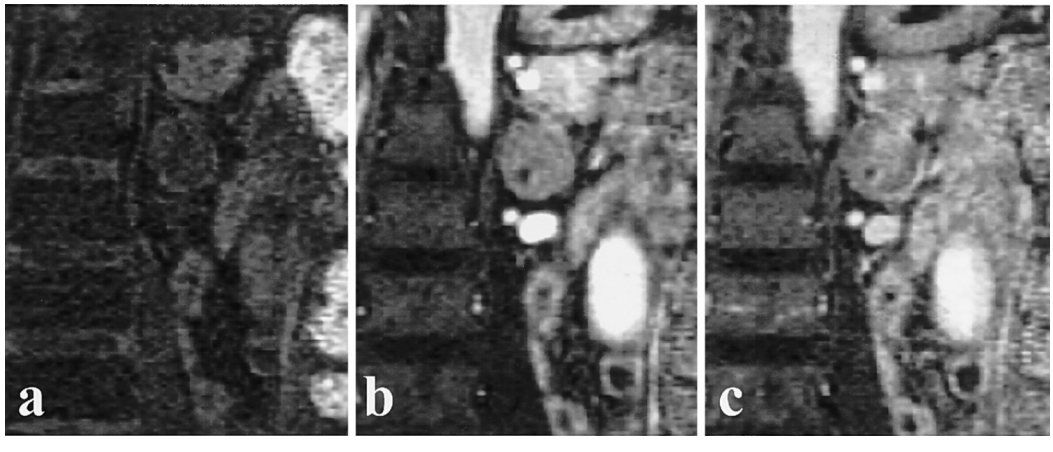

Fig. 7 Adenoma. Dynamic contrast-enhanced images show Type I in the periphery and slow enhancement (Type 4) in the center (before (a), early (b), and delayed (c)). This central region corresponds to degeneration, which shows high signal intensity on T2-weighted images.

Discussion

Most benign non-hyper functioning adrenal adenomas consist of large, lipid-laden cells similar to those of the zona fasciculata. Adenomas can contain variable proportions of cells of the zona reticularis, small cells that appear dark by light microscopy due to their compact, lipid-poor cytoplasm. In some adenomas, the small dark cells of the zona reticularis predominate [13]. Aldosterone-secreting adenomas typically show a proliferation of cells of the zona glomerulosa, small cells with an intermediate number of lipid cytoplasmic inclusions [14]. Most commonly, there is a mixture of cells of the zona fasciculata and zona glomerulosa, but some adenomas are composed entirely of cells of the zona glomerulosa. Thus, both non-hyperfunctioning and hyperfunctioning adenomas can contain highly variable amounts of lipid [15].

Metastases to the adrenal glands reflect the histological features of the primary mass. Therefore, few would be expected to contain lipid in the cytoplasm. However, some masses, such as clear cell subtype renal cell carcinomas, contain cytoplasmic lipid, which can lead to confusion in the evaluation of these masses. Postmortem studies have found that adrenal adenoma occurs more frequently in elderly women, obese persons, diabetics, and patients with carcinoma of the respiratory tract, stomach, prostate, bladder, or kidney [16, 17]. Patients with renal cell carcinoma have 4 times the incidence of adrenal adenoma or hyperplasia compared to the general population. For these reasons, the differential diagnosis of metastases and adenomas in renal cell carcinoma patients is difficult.

Primary adrenal carcinoma can show variable amounts of lipid in the cytoplasm. Well-differentiated adrenal carcinomas can contain lipid in amounts comparable to those found in adenomas, making them difficult to distinguish histological. Pheochromocytomas may occasionally contain normal lipid-rich adrenocortical cells in the mass or may even undergo lipid degeneration.

Many studies have reported the differentiation of adrenal masses based on the CT attenuation value [18–22]. None have reported a malignant adrenal mass with a density of less than 0 HU. If a threshold of greater than 0 HU is set, malignant lesions may be incorrectly identified as adenomas. Such undesirable overlap occurred in 14% of the cases examined with this method.

Leroy-Willig *et al.* [23] have demonstrated that *in vivo* MR spectroscopic imaging is useful for distinguishing between adrenal carcinomas and adenomas based on differences in lipid content. Only one adenoma had lipid content lower than 7%, which overlapped that of the carcinomas. Mitchell *et al.* [8] described the use of chemical shift MR imaging in differentiating between benign adrenal masses and metastases. Tsushima *et al.* [9] reported that adrenal lesions with an SI of less than 5% were metastatic masses or pheochromocytomas, and that adrenal lesions with an SI greater than 5% were adenomas. The characterization of adrenal masses based on the amount of cytoplasmic lipid by pathological examination is not perfect, so other methods for characterization must be developed. Krestin *et al.* [11, 12] reported that dynamic studies after the administration of Gd-DTPA can provide additional information in the delineation and differentiation of adrenal masses. Adenomas showed moderate enhancement and rapid washout, whereas malignant masses and pheochromocytomas showed pronounced enhancement and markedly slower washout (which may be due to increased perfusion and changes in the permeability of capillary vessels). Using this method, the lesions were successfully identified in more than 90% of cases (31 of 34). A dynamic sequence with acquisition at intervals of about 35 sec is needed to evaluate perfusion in greater detail. Our results therefore confirm the findings of earlier studies which showed that both chemical shift and dynamic MR imaging are useful.

Of the 38 adenomas in the present study, 11 contained internal degeneration. All areas of degeneration showed high signal intensity on T2-weighted images (Fig. 6b) and slow enhancement in dynamic MRI studies (Fig. 7). The T1-weighted images showed various signal intensities. Three adenomas were surgically resected and were found to contain areas of absorption and vascularization by histological examination. The radiological findings were suggestive of malignancy in these areas. If a mass showed typical findings of an adenoma in some areas, it was not difficult to distinguish from a malignant mass. However, if an adenoma contained large areas of degeneration and only small areas of adenoma (Figs. 2, 3), it was difficult to identify as an adenoma based on the radiological findings. In such cases, it was not possible to draw an accurate ROI on the lesion, because of the difficulty of distinguishing between non-degenerated and degenerated components.

Chemical shift MRI is an important technique that shows great promise in discriminating between adenomas

and other masses. The images obtained by subtracting in-phase images from opposed-phase images permit lipid in all parts of the mass to be identified easily. The presence of areas of high signal intensity on subtraction images suggests an adenoma.

Dynamic MRI also shows great potential in the differential diagnosis of adrenal masses, but contrast medium must be used in this method, making it more invasive and expensive. Therefore, this method is not suitable for all patients. If the results of the chemical shift MRI clearly indicate adenoma, it is not necessary to perform further examinations. In the present study, 3 adenomas showed a malignant pattern in the dynamic MRI. All of these masses had low SI values (SI = 7, 1, 9), and all were examined using the H15 MR system. For the Vision MR system, all masses with a low SI ($0 < SI < 5$) showed a benign pattern in dynamic MRI studies. These differences were not statistically significant. For the Vision system only, all adenomas with a low SI (identified as non-adenomas in a previous study) showed a benign pattern in dynamic MRI. If an adrenal mass shows a benign pattern in dynamic MRI, it is very likely to be an adenoma, but caution is needed when making this diagnosis, because it could also be a metastasis from HCC (Figs. 4, 5).

Our study has some limitations. First, a pathological diagnosis was not obtained on all of the masses. In particular, other types of masses may be present, although the diagnosis of some of the adenomas did not show change at the prolonged follow-up date. Since 2 different machines (a new one and old one) were used, the results may have been affected by this difference. Because few masses had a low SI ($0 < SI < 5$), it was difficult to determine the usefulness of dynamic MRI over chemical shift MRI.

In conclusion, chemical shift MRI is useful for identifying adenomas in most cases. If an adrenal mass has a low SI, dynamic MRI can also be helpful in the differential diagnosis of adrenal masses.

References

1. Glazer HS, Weyman PJ, Sagel SS, Levitt RG and McClennan BL: Nonfunctioning adrenal masses: Incidental discovery on computed tomography. AJR (1982) 139: 81–85.
2. Bullock WK and Hirst AE: Metastatic carcinoma of the adrenal. Am J Med Sci (1953) 226: 521–524.
3. Abrams HL, Spiro R and Goldstein N: Metastasis in carcinoma: Analysis of 1000 autopsied cases. Cancer (1950) 3: 74–85.
4. Glowset DA: The incidence of metastasis of malignant masses to the adrenals. Am J Cancer (1938) 32: 57–61.
5. Oliver TW Jr, Bernardino ME, Miller JI, Mansour K, Greene D and Davis WA: Isolated adrenal masses in nonsmall-cell bronchogenic carcinoma. Radiology (1984) 153: 217–218.
6. Baker ME, Blinder R, Spritzer C, Leight GS, Herfkens RJ and Dunnick NR: MR evaluation of adrenal masses at 1.5T. AJR (1989) 153: 307–312.
7. Chezmar JL, Robbins SM, Nelson RC, Steinberg HV, Torres WE and Bernardino ME: Adrenal masses: Characterization with T1-weighted MR imaging. Radiology (1988) 166: 357–359.
8. Mitchell DG, Crovello M, Matteucci T, Petersen RO and Miettinen MM: Benign adrenocortical masses: Diagnosis with chemical shift MR imaging. Radiology (1992) 185: 345–351.
9. Tsushima Y, Ishizaka H and Matsumoto M: Adrenal masses: Differentiation with chemical shift, fast low-angle shot MR imaging. Radiology (1993) 186: 705–709.
10. McNicholas MMJ, Lee MJ, Mayo-Smith WW, Hahn PF, Boland GW and Mueller PR: An imaging algorithm for the differential diagnosis of adrenal adenomas and metastases. AJR (1995) 165: 1453–1459.
11. Krestin GP, Steinbrich W and Friedmann G: Adrenal masses: Evaluation with fast gradient-echo MR imaging Gd-DTPA-enhanced dynamic studies. Radiology (1989) 171: 675–680.
12. Krestin GP, Freidmann G Fischback R, Neufang KFR and Allolio B: Evaluation of adrenal masses in oncologic patients: Dynamic contrast-enhanced MR *vs*. CT. J Comput Assist Tomogr (1991) 15: 104–110.
13. O'Hare MJ, Monaghan P and Neville AM: The pathology of adrenocortical neoplasia: A correlated structural and functional approach to the diagnosis of malignant disease. Hum Pathol (1979) 10: 137–154.
14. Gruhn JG and Gould VE: The adrenal glands; in Anderson's Pathology, Kissane JM ed, 9 th Ed, Mosby, St Louis (1990) pp 1580–1619.
15. Reinig JW: MR imaging differentiation of adrenal masses: Has the time finally come? Radiology (1992) 185: 339–340.
16. Whiseand JM, Kostas D and Sommers SC: Some host factors in the development of renal cell carcinoma. West J Med (1962) 70: 284–285.
17. Parker TG and Sommers SC: Adrenal cortical hyperplasia accompanying cancer. Arch Surg (1956) 72: 495–499.
18. Lee MJ, Hahn PF, Papanicolaou N, Egglin TK, Saini S, Mueller PR and Simeone JF: Benign and malignant adrenal masses: CT distinction with attenuation coefficients, size, and observer analysis. Radiology (1991) 179: 415–418.
19. Paivansalo M, Lahde S, Merikanto J and Kallionen M: Computed tomography in primary and secondary adrenal tumours. Acta Radiol (1988) 29: 519–522.
20. van Erkel AR, van Gils APG, Lequin M, Kruitwagen C, Bloem JL and Falke THM: CT and MR distinction of adenomas and nonadenomas of the adrenal gland. J Comput Assist Tomogr (1994) 18: 432–438.
21. Singer AA, Obuchowski NA, Einstein DM and Paushter DM: Metastasis or adenoma? Computed tomographic evaluation of the adrenal mass. Cleve Clin J Med (1994) 61: 200–205.
22. Katz RL and Shirkhoda A: Diagnostic approach to incidental adrenal nodules in the cancer patient: Results of a clinical, radiologic and fine-needle aspiration study. Cancer (1985) 55: 1995–2000.
23. Leroy-Willig A, Bittoun J, Luton JP, Louvel A, Lefevre JE, Bonnin A and Roucayrol JC: *In vivo* MR spectroscopic imaging of the adrenal gland: Distinction between adenomas and carcinomas larger than 15 mm based on lipid content. AJR (1989) 153: 771–773.